J Supercond Nov Magn (2013) 26:2313–2317
DOI 10.1007/s10948-012-1425-4

ORIGINAL PAPER

Structural and Magnetic Properties of the New $La_2SrCo_2FeO_9$ Triple Perovskite

Julio C. Albornoz · David A. Landínez Téllez · Jairo Roa-Rojas · Julian A. Munévar · Elisa Baggio-Saitovich

Received: 21 November 2011 / Accepted: 9 January 2012 / Published online: 5 February 2012

Abstract In this work, we report synthesis and characterization of the new $La_2SrCo_2FeO_9$ triple perovskite material. The samples were produced by the solid-state reaction method. The analyses of the XRD patterns were made by Rietveld refinement through the GSAS code. The results reveal that the material crystallizes in an orthorhombic complex perovskite, space group *Immm (#71)* with lattice parameters $a = 5.4314(3)$ Å, $b = 5.4583(3)$ Å and $c = 7.7018(2)$ Å. SEM micrographs evidence a strongly diffused granular morphology with mean grain size of 2 μm and the EDX spectra show that the chemical composition of samples are in good agreement with the nominal values of the stoichiometric formula. ^{57}Fe Mössbauer spectroscopy recorded at 300 K reveals two sites in concordance with the X-ray diffraction measurements, and its valence state is +3, as determined from the isomer shift found. At 4.2 K magnetic ordering with canting of the Fe moments is found. Measurements of the magnetization as a function of temperature permitted us to determine the ferromagnetic characteristic of material with an effective magnetic moment of $9.7\mu_B$.

Keywords Complex perovskite · Structure · Magnetic properties

J.C. Albornoz · D.A. Landínez Téllez · J. Roa-Rojas (✉)
Grupo de Física de Nuevos Materiales, Departamento de Física, Universidad Nacional de Colombia, AA 5997 Bogotá DC, Colombia
e-mail: jroar@unal.edu.co

J.A. Munévar · E. Baggio-Saitovich
Centro Brasileiro de Pesquisas Físicas, Rua Dr. Xavier Sigaud 150, 22290-180 Rio de Janeiro, RJ, Brasil

1 Introduction

The perovskite oxide materials have been extensively investigated in the last years, because small structural distortions, vacancies and compositional modifications can induce a great variety of physical and chemical properties [1]. When the ideal formula ABO_3 is changed to introduce different types of A and B cations on the octahedral site of the primitive unit cell, the cationic ordering leads to complex perovskites [2]. One of these is known as triple perovskite, which is identified by the $A_2A'B_2B'O_9$ formula. Then, it is possible to produce new materials by the introduction of an alkaline or rare-earth ion in the A, A′ sites and transition metal ions in the B, B′. Depending on the magnetic or electric characteristic of B and B′, it is relatively easy to create new perovskite systems with half-metallic properties [3, 4], magneto-electric response [5] or magnetic ordering [6], which offer promising perspectives in the recent spintronics technology [7].

In order to analyze the possibility to create new magnetic perovskite materials, in this work we report the synthesis, the structural characterization, magnetic studies from magnetization measurements and magnetic and structural properties from ^{57}Fe Mössbauer spectroscopy, of the new ferromagnetic triple perovskite $La_2SrCo_2FeO_9$, which was idealized as the introduction of a lanthanide ion in the A site, an alkaline earth in the A′ and a mixture of two magnetic transition metals in the B and B′ sites of $A_2A'B_2B'O_9$ formula, to construct a triple complex perovskite.

2 Experimental

The samples were synthesized by the solid-state reaction recipe. The precursor powders La_2O_3, $SrCO_3$, Co_2O_3 and

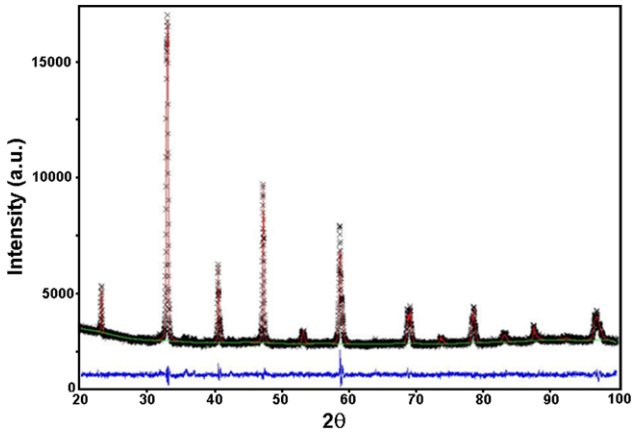

Fig. 1 Characteristic XRD pattern for the triple perovskite $La_2SrCo_2FeO_9$. *Symbols* represent experimental diffraction data and base line is the difference between experimental and simulated patterns (*continuous line*)

Fe_3O_4 (Aldrich 99.9%) were mixed in stoichiometric proportions according to the chemical formula $La_2SrCo_2FeO_9$. Mixture was ground to form a pellet and annealed at 1250 °C for 12 hours. The samples were then reground, repelletized and sintered at 1250 °C for 24 hours and 1350 °C for 24 hours. X-ray diffraction (XRD) experiment was performed by means a *PW1710* diffractometer with $\lambda_{CuK\alpha} = 1.54064$ Å. Rietveld refinement of the diffraction pattern was made by the GSAS code [8]. Scanning Electron Microscopy (SEM) images were obtained by using a FEI QUANTA 200 microscopy, which has a system for Energy Dispersive X-ray (EDX) analysis. Field cooling measurements of susceptibility as a function of temperature and magnetization as a function of applied field were carried out by using a MPMS Quantum Design SQUID. ^{57}Fe Mössbauer spectra were taken at room temperature and at 4.2 K using a 50 mCi ^{57}Co:Rh source in transmission configuration, kept at the same temperature of the sample, in sinusoidal movement. The isomer shift is relative to that of α-Fe.

3 Results and Discussion

The analysis of XRD pattern showed in Fig. 1 reveals the presence of characteristic peaks of complex perovskite systems. In Fig. 1, crosses represent the experimental data and the line corresponds to simulated pattern by means of GSAS code. The base line is the difference between theoretical and experimental results.

Rietveld refinement permitted to establish that this material crystallizes in a orthorhombic triple perovskite with space group *Immm (#71)* and lattice constants are $a = 5.4314(3)$ Å, $b = 5.4583(3)$ Å and $c = 7.7018(2)$ Å. These results are 99.78%, in agreement with the theoretical values obtained from the Structure Prediction Diagnostic Software *SPuDS* [9], which predicts that lattice constants $a = 5.458(8)$ Å, $b = 5.427(1)$ Å and $c = 7.688(9)$ Å for the $La_2SrCo_2FeO_9$ material.

Table 1 Atomic positions and occupancy for the $La_2SrCo_2FeO_9$

Ion	*x*	*y*	*z*	Occupancy
Sr	0.5000	0.0000	0.2476	0.3379
La	0.5000	0.0000	0.2476	0.6804
Co(1)	0.0000	0.0000	0.0000	0.6025
Fe(1)	0.0000	0.0000	0.0000	0.4371
Co(1)	0.5000	0.5000	0.0000	0.7491
Fe(2)	0.5000	0.5000	0.0000	0.2015
O(1)	0.2295	0.2809	0.0000	1.7620
O(2)	0.0000	0.0000	0.2509	1.3551

The parameters of the refinement are: $R_F^2 = 2.67\%$; $x^2 = 1.313$; $R_{WP} = 3.82\%$ and $R_P = 3.20\%$. The numeric results of atomic positions and occupancy obtained from the Rietveld analysis are shown in Table 1.

One important parameter in perovskite materials is the tolerance factor, which is related to the probability of formation of octahedral coordination of B and B′ cations with the oxygen anion. The tolerance factor calculated for the $La_2SrCo_2FeO_9$ complex perovskite was 0.982, which is characteristic of perovskite-like lattices distorted from the ideal cubic structure of triple $A_2A'B_2B'O_9$. From the Rietveld refinement the values for the bond distances and positions of cations relative to the neighbor ions were obtained (Table 2).

The surface morphology of $La_2SrCo_2FeO_9$ samples was studied by SEM images as shown in Fig. 2. The analysis performed reveals the occurrence of granular topology with different grain sizes. As observed in the microphotography, grains are strongly diffused between them, but great empty spaces appear too. It is important to notice that the sample evidences a single type of grain. From the EDX semi-quantitative analysis, which considers the spectrum areas for each element showed in Fig. 3, we obtain the experimental composition of material. These values were compared with the theoretical composition, calculated from the $La_2SrCo_2FeO_9$ stoichiometric formula. Results are presented in Table 3.

The results of Fig. 3 and Table 3 corroborate with 97% that there exists a single phase, which corresponds to the stoichiometry of $La_2SrCo_2FeO_9$. From structural, morphologic and compositional characterizations we deduced that no other crystallographic phases or impurities are present in the samples.

The ^{57}Fe Mössbauer spectra were fitted through the NORMOS software, using the Full Hamiltonian Site anal-

Table 2 Inter-atomic distances and positions of cations relative to Sr ions

Vector	Length (Å)	Neighbor	Atom	Coordin.
Sr_Sr	3.793(35)	0.50000	0.00000	−0.24630
Sr_Sr	3.907(35)	0.50000	0.00000	0.75370
Sr_Sr	3.8506(5)	−0.50000	0.25370	
Sr_Sr	3.8506(5)	0.00000	0.50000	0.25370
Sr_Sr	3.8506(5)	−0.50000	0.25370	
Sr_Sr	3.8506(5)	1.00000	0.50000	0.25370
Sr_La	0.008(19)	0.50000	0.00000	0.24737
Sr_La	3.802(18)	0.50000	0.00000	−0.24737
Sr_La	3.899(18)	0.50000	0.00000	0.75262
Sr_La	3.85049(22)	−0.50000	0.25262	
Sr_La	3.85049(22)	0.00000	0.50000	0.25262
Sr_La	3.85049(22)	−0.50000	0.25262	
Sr_La	3.85049(22)	1.00000	0.50000	0.25262
Sr_Co1	3.312(10)	0.00000	0.00000	0.00000
Sr_Co1	3.312(10)	1.00000	0.00000	0.00000
Sr_Co1	3.356(10)	−0.50000	0.50000	
Sr_Co1	3.356(10)	0.50000	0.50000	0.50000
Sr_Fe1	3.312(10)	0.00000	0.00000	0.00000
Sr_Fe1	3.312(10)	1.00000	0.00000	0.00000
Sr_Fe1	3.356(10)	−0.50000	0.50000	
Sr_Fe1	3.356(10)	0.50000	0.50000	0.50000
Sr_Co2	3.324(10)	−0.50000	0.00000	
Sr_Co2	3.324(10)	0.50000	0.50000	0.00000
Sr_Co2	3.345(10)	0.50000		
Sr_Co2	3.345(10)	0.00000	0.50000	
Sr_Fe2	3.324(10)	−0.50000	0.00000	
Sr_Fe2	3.324(10)	0.50000	0.50000	0.00000
Sr_Fe2	3.345(10)	0.50000		
Sr_Fe2	3.345(10)	0.00000	0.50000	
Sr_O1	2.879(16)	0.22630	0.28853	0.00000
Sr_O1	2.879(16)	0.77370	0.28853	0.00000
Sr_O1	2.879(16)	0.22630	−0.28853	0.00000
Sr_O1	2.879(16)	0.77370	−0.28853	0.00000
Sr_O1	2.581(16)	−0.21147	0.50000	
Sr_O1	2.581(16)	−0.21147	0.50000	
Sr_O1	2.581(16)	0.72630	0.21147	0.50000
Sr_O1	2.581(16)	0.27370	0.21147	0.50000
Sr_O2	2.7159(6)	0.00000	0.00000	0.25024
Sr_O2	2.7159(6)	1.00000	0.00000	0.25024
Sr_O2	2.7294(5)	−0.50000	0.24976	
Sr_O2	2.7294(5)	0.50000	0.50000	0.24976

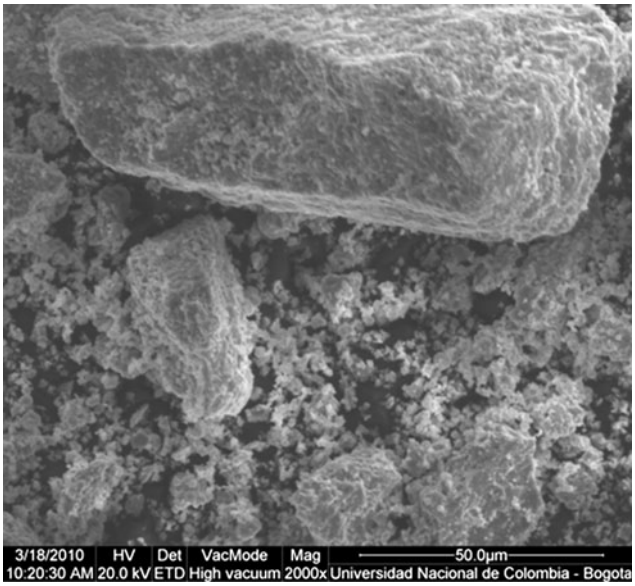

Fig. 2 SEM micrograph of $La_2SrCo_2FeO_9$ obtained from ETD detector (secondary electrons)

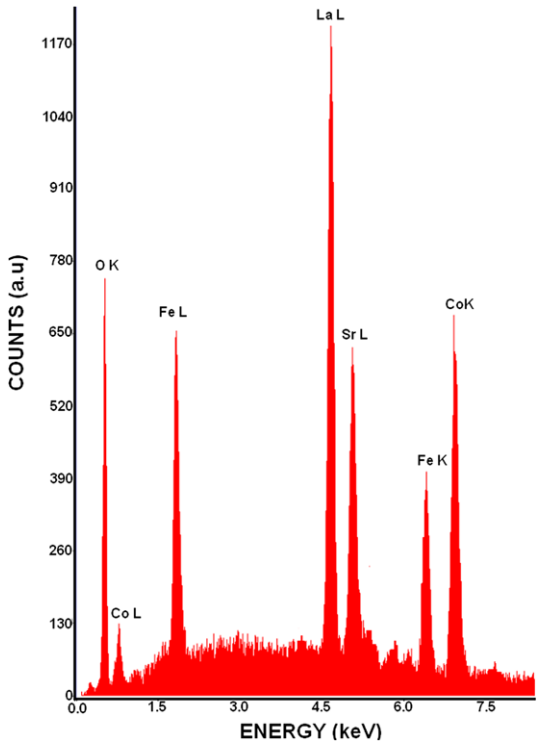

Fig. 3 EDX spectrum for $La_2SrCo_2FeO_9$. It is observed in the picture that there are not traces of impurities

ysis. The spectrum taken at room temperature revealed only an absorption peak, which indicates that there are no impurities, as was shown through X-ray diffraction measurements. This absorption peak, however, is somewhat broad and asymmetric, indicating different environments for the Fe atom in the lattice. We fitted this absorption peak with two quadrupole doublets, keeping fixed the line width to $\Gamma = 0.251$ mm/s, and we found the hyperfine parameters shown in Table 4.

The proportion in area for each site is roughly 50%, each site relative to each crystallographic site found through the

Table 3 Results of semi quantitative EDX analysis for $La_2SrCo_2FeO_9$ samples

Atom	Theor. %Wt	Exper. %Wt
La	40.67	41.89
Sr	12.83	13.21
Co	17.25	17.77
Fe	8.17	8.41
O	21.08	18.72

Table 4 ^{57}Fe Mössbauer parameters for the spectra at 296 K and at 4.2 K for $La_2SrCo_2FeO_9$ powdered sample

T (K)	Site	δ (mm/s)	Γ_{QS} (mm/s)	B (T)
300	1	0.25(1)	0.39(1)	–
	2	0.23(1)	0.16(1)	–
4.2	1	0.28(1)	0.43(1)	50.96(1)
	2	0.26(1)	0.20(1)	48.24(1)

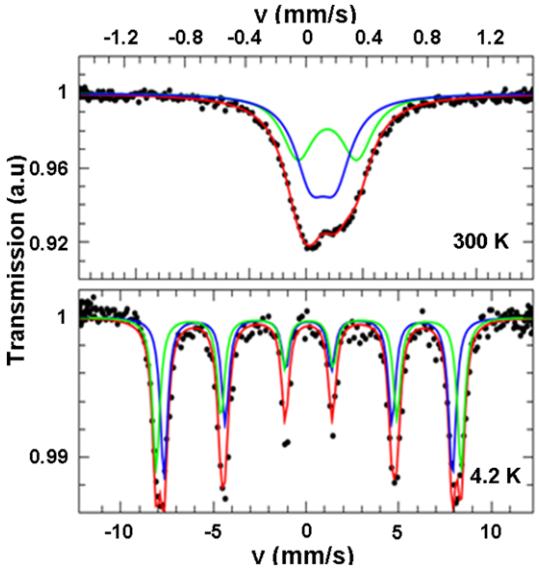

Fig. 4 ^{57}Fe Mössbauer spectra measured at 300 K and at 4.2 K, exhibiting two sites for Fe in the paramagnetic and magnetic phase

Rietveld refinement; the difference in occupancy for Fe in each crystallographic site can be reflected in the quadrupole splitting for each site, minor differences in occupancy can represent a minor change in the electric field gradient that interacts with the Fe quadrupole moment in its nuclear excited state ($I = 3/2$). The isomer shift is roughly the same for both sites, indicating same valence. These values reflect most likely a high spin Fe^{3+} valence, compatible with the fact that the Sr^{2+} doping on La^{3+} site will increase the volume of the lattice, being crystallographically more favorable a high spin Fe ion configuration. A mixed valence for Fe should have been expected, since the substitution in the perovskite A site would lead to charge imbalance [10], but the combination of Fe and Co atoms in the B site compensates it. This means that we must take +3.5 for the valence of Co atoms, which means Co^{3+} and a Co^{4+} ions.

In Fig. 4 the Mössbauer spectrum of $La_2SrCo_2FeO_9$ at 4.2 K reveals a well developed magnetic sextet, indicating magnetic ordering at lower temperatures, probably due to localization of moments and interaction via exchange mechanism.

This spectrum was fitted with two magnetic sites, equivalent to the sites found previously for RT spectrum. The values of the isomer shift and quadrupole splitting are different from the RT values due to thermal effects. No structural phase transition is evident, since there is not found a remarkably high variation in the quadrupole interaction $eQV_{ZZ}/2$, the energy term in the Hamiltonian that depends on lattice and electronic characteristics of the Fe environment. The line widths for these sites are somewhat broad ($\Gamma = 0.481$ mm/s), probably related to small lattice inhomogeneities that could lead to inhomogeneous magnetic ordering or slightly inequivalent sites. The magnitude of the hyperfine fields confirms that Fe is in +3 valence state. The difference in magnetic hyperfine fields for the sites fitted is 3 T, as can be inferred from Table 4. We take the main component of the electric field gradient at the Fe sites, V_{ZZ}, to be in the c crystallographic direction. The angle that makes the magnetic hyperfine field with c axis within this model is close to 60 degrees for both sites, confirming an inhomogeneous alignment of the Fe moments. These results can be understood as follows: the Fe moments are canted with respect to c crystallographic axis, probably due to the interaction with Co moments. The approximate magnetic moment per Fe for each site is $3.40\mu_B$ and $3.22\mu_B$, with an average magnetic moment of $3.31\mu_B$.

The magnetic properties of $La_2SrCo_2FeO_9$ have been investigated by measuring the DC susceptibility in the temperature range from 2 to 300 K and at an applied magnetic field of 50 Oe. Figure 5 shows the dependence of the susceptibility on temperature for $La_2SrCo_2FeO_9$ when it is measured using the Zero Field Cooling and Field Cooling recipes.

The fitting susceptibility as a function of temperature was made by the Curie–Weiss equation,

$$\chi = \chi_0 + \frac{C}{T - T_C}, \tag{1}$$

which had permitted us to establish the ferromagnetic character of material with a Curie temperature $T_C = 123.3$ K, a Curie constant $C = 11.7438$ emu·K/mol and a susceptibility independent of temperature of $\chi_0 = 2.56 \times 10^{-2}$ emu/mol. From the Curie constant we obtain the effective magnetic moment of material $\mu_{eff} = 9.7\mu_B$. Theoretical calculations by the Hund rule, with $P_{eff} = g\sqrt{J(J+1)}$, predict that magnetic moments of the isolated ions Co^{4+}

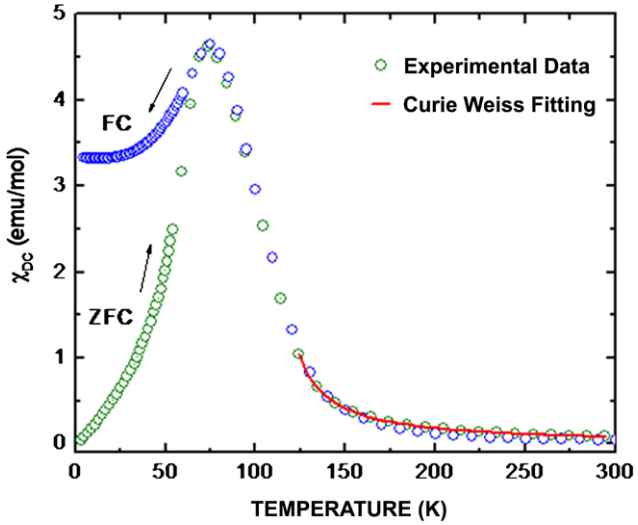

Fig. 5 Measurements of ZFC and FC susceptibility as a function of temperature for $La_2SrCo_2FeO_9$

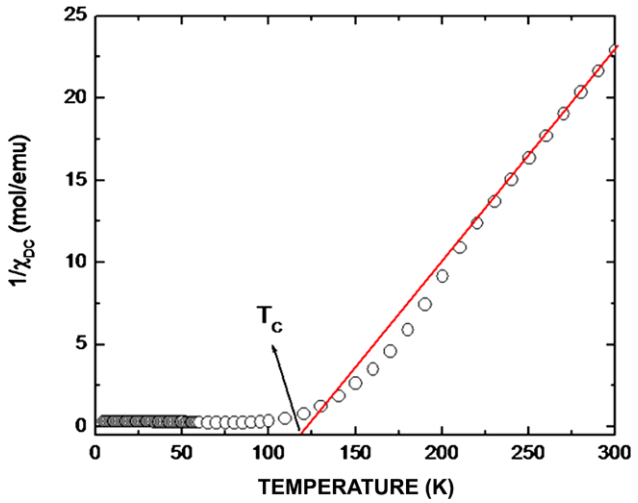

Fig. 6 High temperature linear fit of $1/\chi$ as a function of temperature for $La_2SrCo_2FeO_9$

and Fe^{2+} must be $\mu_{Co}^{4+} = 3.87\mu_B$ and $\mu_{Fe}^{2+} = 5.5\mu_B$, respectively [10]. The effective magnetic moment of $La_2SrCo_2FeO_9$ is obtained to be $\mu_{eff} = 9.33\mu_B$, where we have used $\mu_{eff} = \sqrt{\mu_{Co^{4+}}^2 + \mu_{Fe^{2+}}^2}$, by considering two Co^{4+} cations in the crystallographic unit cell. This result corresponds to 96% agreement between experimental and theoretical values.

In order to verify the ferromagnetic behavior of the $La_2SrCo_2FeO_9$ triple perovskite, in Fig. 6 we show the curve of $1/\chi$ as a function of temperature. In the picture, the value of T_C is corroborated by the extrapolation of the high temperature linear-like behavior on the temperature axis.

4 Conclusions

The synthesis and structural characterization of the new $La_2SrCo_2FeO_9$ perovskite-like material was performed. The Rietveld analyses reveal that this material crystallizes in an orthorhombic complex perovskite which corresponds to *Immm (#71)* space group. ^{57}Fe Mössbauer spectroscopy revealed two sites for iron, both with valence +3 for Fe, and magnetic ordering at 4.2 K. Measurements of the magnetic susceptibility showed a ferromagnetic ordering transition for $T_C = 123.3$ K, which was fitted by the Curie–Weiss model. From the fitting we obtain the magnetic moment of the unit cell to be $\mu = 9.7\mu_B$.

Acknowledgements This work was partially supported by Division of Investigations (National University of Colombia, Bogotá DC) and Brazilian agency CNPq.

References

1. Hazen, R.M.: Sci. Am. **258**, 54 (1988)
2. Ortiz Diaz, O., Jayro Arbey Rodriguez, M., Fajardo, F., Landínez Téllez, D.A., Roa-Rojas, J.: Physica B **398**, 248 (2007)
3. Philips, J.B., Majewski, P., Alff, L., Gross, R., Graf, T., Branst, M.S., Simon, J., Walther, T., Mader, W., Topwal, D., Sarma, D.D.: Phys. Rev. B **68**, 144431 (2003)
4. Palkar, V.R., Malik, S.K.: Solid State Commun. **134**, 783 (2005)
5. Lofland, S.E., Scabarozi, T., Moritomo, Y., Xu, Sh.: J. Magn. Magn. Mater. **260**, 181 (2003)
6. Di Trolio, A., Larciprete, R., Testa, A.M., Fiorani, D., Imperatori, P., Turchini, S., Zema, N.: J. Appl. Phys. **100**, 13907 (2006)
7. Larson, A.C., Von Dreele, R.B.: General Structure Analysis System (GSAS). Los Alamos National Laboratory Report LAUR, pp. 86–748 (2000)
8. Lufaso, M.W., Woodward, P.M.: Prediction of the crystal structures of perovskites using the software program spuds. Acta Crystallogr., B Struct. Crystallogr. Cryst. Chem. **57**, 725 (2001)
9. Neov, L., Dabrowski Hofmann, M., Bouwmeester, H.J.M.: Appl. Phys. A **74**, S664 (2002)
10. Kittel, C.: Introduction to Solid State Physics, 8th edn. University of California, Berkeley (2005)